Measurements of $\mathcal{B}\left(\overline{B}^0 \to \Lambda_c^+ \bar{p}\right)$ and $\mathcal{B}\left(B^- \to \Lambda_c^+ \bar{p}\pi^-\right)$ and studies of $\Lambda_c^+\pi^-$ resonances by BaBar Collaboration – contents analysis

Kerim Guseynov

Based on `arXiv:0807.4974`

Faculty of Physics
Moscow State University

Nov 18, 2022

Introduction

- Complementary measurements to heavy baryon decays,
- Baryon production mechanisms:
  suppression of decays like $B \to p\bar{p}$ vs $B \to p\bar{p}\pi$,
- Scalar mesons simplify spin measurements,

BaBar detector and data sample

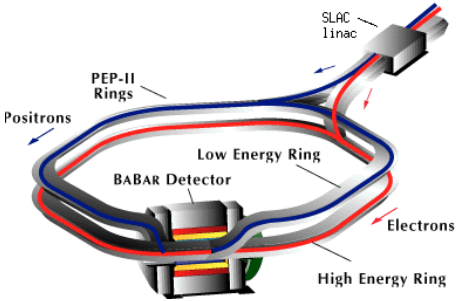

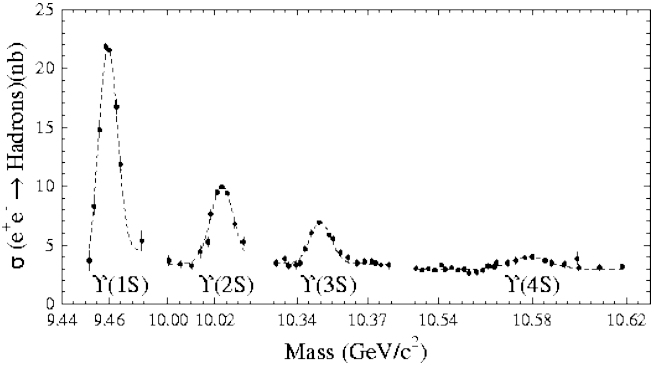

383 million $\Upsilon(4S) \to B\overline{B}$ decays

- Vertex tracker
- Drift chamber
- Cherenkov detector

Λ_c^+ reconstruction. Background. Simulation. Efficiencies

TABLE I: Detection efficiency for $\overline{B}^0 \to \Lambda_c^+ \overline{p}$ signal events, determined from signal Monte Carlo samples and separated by Λ_c^+ decay mode. The numbers correspond to the efficiency for $\overline{B}^0 \to \Lambda_c^+ \overline{p}$ ($B^- \to \Lambda_c^+ \overline{p}\pi^-$), $\Lambda_c^+ \to f_l$, where f_l is a given final state. The efficiencies quoted for the $B^- \to \Lambda_c^+ \overline{p}\pi^-$ decays are averaged across phase space.

	Efficiency for $\Lambda_c^+ \to f_l$	
f_l	$\overline{B}^0 \to \Lambda_c^+ \overline{p}$	$B^- \to \Lambda_c^+ \overline{p}\pi^-$
$pK^-\pi^+$	22.9%	15.4%
pK_S^0	21.6%	14.3%
$pK_S^0\pi^+\pi^-$	9.6%	5.6%
$\Lambda\pi^+$	17.2%	11.6%
$\Lambda\pi^+\pi^-\pi^+$	–	4.0%

Signal extraction

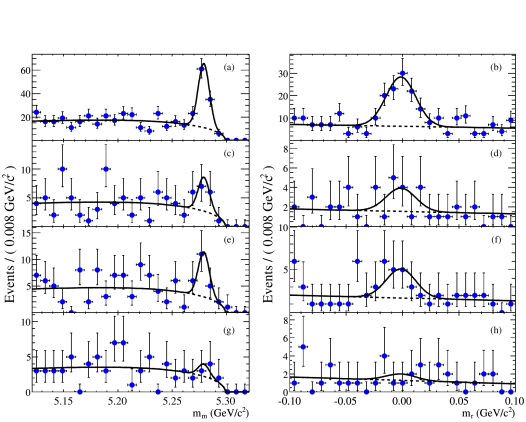

FIG. 1: Projections of m_m (left) and m_r (right) in data for $\overline{B}^0 \to \Lambda_c^+ \overline{p}$ candidates, separated by Λ_c^+ decay mode: (a, b) are $\Lambda_c^+ \to pK^-\pi^+$, (c, d) are $\Lambda_c^+ \to pK_S^0$, (e, f) are $\Lambda_c^+ \to pK_S^0\pi^+\pi^-$, and (g, h) are $\Lambda_c^+ \to \Lambda\pi^+$. The m_m projections (a, c, e, g) are for $|m_r| < 0.030$ GeV/c^2 and the m_r projections (b, d, f, h) are for $m_m > 5.27$ GeV/c^2. The solid curves correspond to the PDF from the simultaneous 2-D fit to candidates for the four Λ_c^+ decay modes, and the dashed curves represent the background component of the PDF.

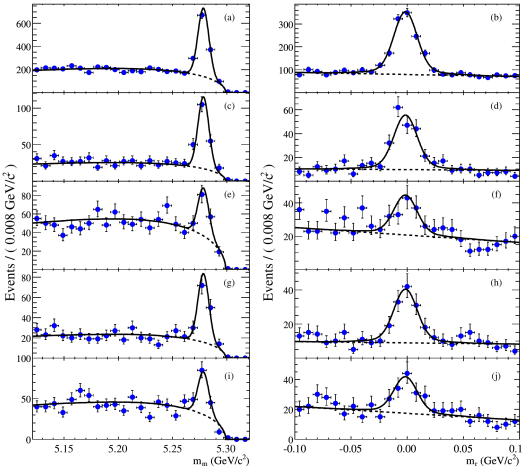

FIG. 2: Projections of m_m (left) and m_r (right) in data for $B^- \to \Lambda_c^+ \overline{p}\pi^-$ candidates, separated by Λ_c^+ decay mode: (a, b) are $\Lambda_c^+ \to pK^-\pi^+$, (c, d) are $\Lambda_c^+ \to pK_S^0$, (e, f) are $\Lambda_c^+ \to pK_S^0\pi^+\pi^-$, (g, h) are $\Lambda_c^+ \to \Lambda\pi^+$, and (i, j) are $\Lambda_c^+ \to \Lambda\pi^+\pi^-\pi^+$. The m_m projections (a, c, e, g, i) are for $|m_r| < 0.030$ GeV/c^2 and the m_r projections (b, d, f, h, j) are for $m_m > 5.27$ GeV/c^2. The solid curves correspond to the PDF from the simultaneous 2-D fit to candidates for the five Λ_c^+ decay modes, and the dashed curves represent the background component of the PDF.

Fit results

TABLE II: Signal yields from simultaneous fits (across Λ_c^+ decay modes) to $\overline{B}^0 \to \Lambda_c^+ \overline{p}$ and $B^- \to \Lambda_c^+ \overline{p}\pi^-$ candidates.

	N_{sig}	
Mode	$\overline{B}^0 \to \Lambda_c^+ \overline{p}$	$B^- \to \Lambda_c^+ \overline{p}\pi^-$
$pK^-\pi^+$	90 ± 11	991 ± 45
pK_S^0	10 ± 4	165 ± 15
$pK_S^0\pi^+\pi^-$	14 ± 5	86 ± 14
$\Lambda\pi^+$	3 ± 3	114 ± 13
$\Lambda\pi^+\pi^-\pi^+$	–	88 ± 13

Efficiency correction

$$\mathcal{B}\left(\overline{B}^0 \to \Lambda_c^+ \bar{p}\right)_l = \frac{N_{\mathrm{sig},\,l}}{N_{B\overline{B}} \cdot \varepsilon_l \cdot \mathcal{R}_l \cdot \mathcal{B}\left(\Lambda_c^+ \to pK^-\pi^+\right)}$$

$$\mathcal{B}\left(B^- \to \Lambda_c^+ \bar{p}\pi^-\right)_l = \frac{0.99 \cdot \left(\sum\limits_i \frac{{}^s W_i}{\varepsilon_i}\right)}{N_{B\overline{B}} \cdot \mathcal{R}_l \cdot \mathcal{B}\left(\Lambda_c^+ \to pK^-\pi^+\right)}$$

TABLE III: Summary of the individual and combined branching fraction measurements for $\overline{B}^0 \to \Lambda_c^+ \overline{p}$ and $B^- \to \Lambda_c^+ \overline{p}\pi^-$. The uncertainties are statistical, systematic, and due to $\mathcal{B}(\Lambda_c^+ \to pK^-\pi^+)$, respectively.

Mode	$\mathcal{B}(\overline{B}^0 \to \Lambda_c^+ \overline{p})$	$\mathcal{B}(B^- \to \Lambda_c^+ \overline{p}\pi^-)$
$\Lambda_c^+ \to pK^-\pi^+$	$(2.05 \pm 0.25 \pm 0.05 \pm 0.53) \times 10^{-5}$	$(3.38 \pm 0.13 \pm 0.11 \pm 0.88) \times 10^{-4}$
$\Lambda_c^+ \to pK_S^0$	$(1.49 \pm 0.60 \pm 0.17 \pm 0.39) \times 10^{-5}$	$(3.82 \pm 0.35 \pm 0.38 \pm 0.99) \times 10^{-4}$
$\Lambda_c^+ \to pK_S^0\pi^+\pi^-$	$(4.33 \pm 1.55 \pm 0.57 \pm 1.13) \times 10^{-5}$	$(4.58 \pm 0.70 \pm 0.66 \pm 1.19) \times 10^{-4}$
$\Lambda_c^+ \to \Lambda\pi^+$	$(0.71 \pm 0.71 \pm 0.18 \pm 0.18) \times 10^{-5}$	$(3.98 \pm 0.45 \pm 0.39 \pm 1.03) \times 10^{-4}$
$\Lambda_c^+ \to \Lambda\pi^+\pi^-\pi^+$	–	$(3.49 \pm 0.51 \pm 0.38 \pm 0.91) \times 10^{-4}$
combined	$(1.89 \pm 0.21 \pm 0.06 \pm 0.49) \times 10^{-5}$	$(3.38 \pm 0.12 \pm 0.12 \pm 0.88) \times 10^{-4}$

Efficiency correction

$$\mathcal{B}\left(\overline{B}^0 \to \Lambda_c^+ \bar{p}\right)_l = \frac{N_{\mathrm{sig},\,l}}{N_{B\overline{B}} \cdot \varepsilon_l \cdot \mathcal{R}_l \cdot \mathcal{B}\left(\Lambda_c^+ \to pK^-\pi^+\right)}$$

$$\mathcal{B}\left(B^- \to \Lambda_c^+ \bar{p}\pi^-\right)_l = \frac{0.99 \cdot \left(\sum_i \frac{{}^s W_i}{\varepsilon_i}\right)}{N_{B\overline{B}} \cdot \mathcal{R}_l \cdot \mathcal{B}\left(\Lambda_c^+ \to pK^-\pi^+\right)}$$

TABLE III: Summary of the individual and combined branching fraction measurements for $\overline{B}^0 \to \Lambda_c^+ \overline{p}$ and $B^- \to \Lambda_c^+ \overline{p}\pi^-$. The uncertainties are statistical, systematic, and due to $\mathcal{B}(\Lambda_c^+ \to pK^-\pi^+)$, respectively.

Mode	$\mathcal{B}(\overline{B}^0 \to \Lambda_c^+ \overline{p})$	$\mathcal{B}(B^- \to \Lambda_c^+ \overline{p}\pi^-)$
$\Lambda_c^+ \to pK^-\pi^+$	[illegible]	$\pm 0.88) \times 10^{-4}$
$\Lambda_c^+ \to pK_S^0$	$\frac{\mathcal{B}\left(B^- \to \Lambda_c^+ \bar{p}\pi^-\right)}{\mathcal{B}\left(\overline{B}^0 \to \Lambda_c^+ \bar{p}\right)} = 15.4 \pm 1.8 \pm 0.3$	$\pm 0.99) \times 10^{-4}$
$\Lambda_c^+ \to pK_S^0\pi^+$		$\pm 1.19) \times 10^{-4}$
$\Lambda_c^+ \to \Lambda\pi^+$		$\pm 1.03) \times 10^{-4}$
$\Lambda_c^+ \to \Lambda\pi^+\pi^-\pi^+$	–	$(3.49 \pm 0.51 \pm 0.38 \pm 0.91) \times 10^{-4}$
combined	$(1.89 \pm 0.21 \pm 0.06 \pm 0.49) \times 10^{-5}$	$(3.38 \pm 0.12 \pm 0.12 \pm 0.88) \times 10^{-4}$

Systematic uncertainties

TABLE IV: Summary of the contributions to the relative systematic uncertainty in $\mathcal{B}(\overline{B}^0 \to \Lambda_c^+ \overline{p})$ for each Λ_c^+ decay mode. The total for each mode is determined by adding the uncertainty from each source in quadrature. The fractional statistical uncertainty in the fit yield for each mode is provided for comparison.

Source	$\overline{B}^0 \to \Lambda_c^+ \overline{p}$ Systematic Uncertainty			
	$\Lambda_c^+ \to pK^-\pi^+$	$\Lambda_c^+ \to pK_S^0$	$\Lambda_c^+ \to pK_S^0\pi^+\pi^-$	$\Lambda_c^+ \to \Lambda\pi^+$
$B\overline{B}$ events	1.1%	1.1%	1.1%	1.1%
$\mathcal{R}_l$	–	8.5%	11.8%	8.9%
MC statistics	0.4%	0.6%	0.6%	0.4%
Tracking	1.7%	1.9%	2.8%	1.7%
Displaced Vertices	–	1.1%	1.1%	1.1%
Particle Identification	1.5%	2.1%	1.7%	1.6%
Fitting	0.9%	7.0%	4.9%	24.2%
Total	3%	12%	13%	26%
Statistical	12%	40%	36%	100%

Source	$B^- \to \Lambda_c^+ \overline{p}\pi^-$ Systematic Uncertainty				
	$\Lambda_c^+ \to pK^-\pi^+$	$\Lambda_c^+ \to pK_S^0$	$\Lambda_c^+ \to pK_S^0\pi^+\pi^-$	$\Lambda_c^+ \to \Lambda\pi^+$	$\Lambda_c^+ \to \Lambda\pi^+\pi^-\pi^+$
$B\overline{B}$ events	1.1%	1.1%	1.1%	1.1%	1.1%
$\mathcal{R}_l$	–	8.5%	11.8%	8.9%	6.1%
MC statistics	0.6%	2.1%	3.1%	2.0%	3.0%
Tracking	2.6%	2.3%	3.2%	2.1%	2.9%
Displaced Vertices	–	1.1%	1.1%	1.1%	1.1%
Particle Identification	0.8%	1.8%	2.5%	1.8%	3.5%
Fitting	1.6%	3.2%	6.5%	2.5%	2.4%
Total	3.4%	9.9%	14.5%	10.0%	8.7%
Statistical	4.5%	9.1%	16.3%	11.4%	14.8%

Resonant structure of $B^- \to \Lambda_c^+ \bar{p}\pi^-$: $\Sigma_c(2455)^0$

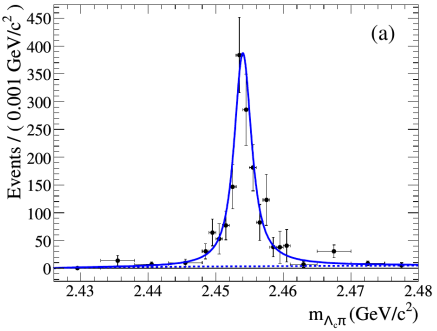

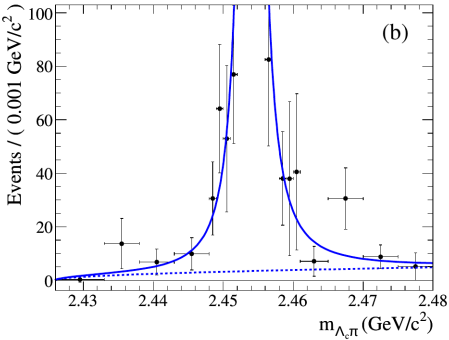

Fit parameter	Value	PDG value
$Y_{\rm sig}$	1522 ± 149	–
m_R (MeV/c^2)	2454.0 ± 0.2	2453.8 ± 0.2
Γ_R (MeV)	2.6 ± 0.5	2.2 ± 0.4

Resonant structure of $B^- \to \Lambda_c^+ \bar{p}\pi^-$: $\Sigma_c(2520)^0$ – no signal

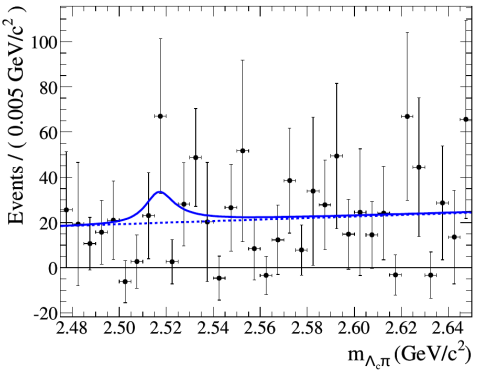

$$Y_{\rm sig} = 27 \pm 69$$

FIG. 6: Projection of $m_{\Lambda_c\pi}$ in the region of the $\Sigma_c(2520)^0$ resonance. Events are efficiency corrected and weighted using the ${}_s\mathcal{P}lot$ technique, and the result of a binned χ^2 fit to a relativistic D-wave Breit-Wigner signal with a mass-dependent width plus a linear background is overlaid. The bin size is $5\,\mathrm{MeV}/c^2$. No significant signal is seen.

Resonant structure of $B^- \to \Lambda_c^+ \bar{p}\pi^-$: $\Sigma_c(2800)^0$

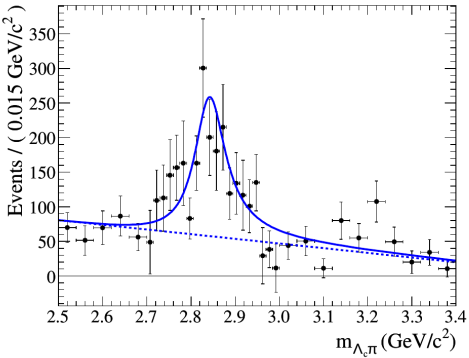

FIG. 7: Projection of $m_{\Lambda_c\pi}$ showing an excited Σ_c^0 resonance. Events are efficiency corrected and weighted using the ${}_s\mathcal{P}lot$ technique. The result of a binned χ^2 fit to a relativistic D-wave Breit-Wigner signal with a mass-dependent width plus a linear background is overlaid. The variable bin sizes range from 15 to 40 MeV/c^2.

Fit parameter	Value	PDG value
$Y_{\rm sig}$	1449 ± 284	–
m_R (MeV/c^2)	2846 ± 8	2802^{+4}_{-7}
Γ_R (MeV)	86^{+33}_{-22}	61^{+28}_{-18}

5.8σ significance

5.2σ with systematics

Systematic uncertainties of resonance parameters

TABLE VIII: Systematic uncertainties for $Y_{\rm sig}$, m_R (in MeV/c^2), and Γ_R (in MeV) for the $\Sigma_c(2455)^0$ and excited Σ_c^0 resonances.

	$\Sigma_c(2455)^0$		excited Σ_c^0		
Systematic Source	$Y_{\rm sig}$	Γ_R	$Y_{\rm sig}$	m_R	Γ_R
Resonant Signal PDF	–	–	5.9%	–	$\pm$ 7
Non-resonant Signal PDF	–	–	1.2%	–	$\pm$ 2
Binning	6.9%	$\pm$0.3	20%	$\pm$10	$\pm$10
Total	6.9%	$\pm$0.3	21%	$\pm$10	$\pm$12

Resonant structure of $B^- \to \Lambda_c^+ \bar{p}\pi^-$: Branching ratios

$$\frac{\mathcal{B}\left(B^- \to \Sigma_c(2455)^0 \bar{p}\right)}{\mathcal{B}\left(B^- \to \Lambda_c^+ \bar{p}\pi^-\right)} = (12.3 \pm 1.2 \pm 0.8) \times 10^{-2}$$

$$\frac{\mathcal{B}\left(B^- \to \Sigma_c(2800)^0 \bar{p}\right)}{\mathcal{B}\left(B^- \to \Lambda_c^+ \bar{p}\pi^-\right)} = (11.7 \pm 2.3 \pm 2.4) \times 10^{-2}$$

$$\frac{\mathcal{B}\left(B^- \to \Sigma_c(2520)^0 \bar{p}\right)}{\mathcal{B}\left(B^- \to \Lambda_c^+ \bar{p}\pi^-\right)} < 0.9 \times 10^{-2} \text{ (90\% C.L.)}$$

$\Sigma_c(2455)$ spin measurement

$B^- \to \Sigma_c(2455)^0\big(\to \Lambda_c^+\pi^-\big)\bar{p}$: θ_h is the angle between Λ_c^+ and $\bar{p}$ in $\Sigma_c(2455)^0$ rest frame.

Ideal distributions for $J^P = 1/2$ and $3/2$:

$$J^P(\Sigma_c(2455)^0) = \frac{1}{2}: \quad \frac{\mathrm{d}N}{\mathrm{d}\cos\theta_h} \propto 1$$

$$J^P(\Sigma_c(2455)^0) = \frac{3}{2}: \quad \frac{\mathrm{d}N}{\mathrm{d}\cos\theta_h} \propto 1 + 3\cos^2\theta_h$$

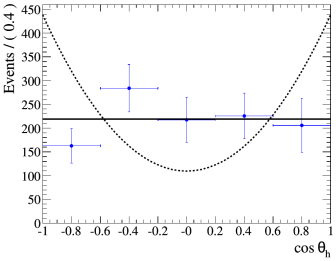

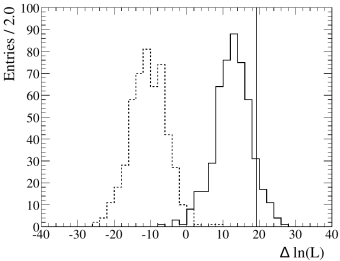

Conclusions

- $\overline{B}^0 \to \Lambda_c^+ \bar{p}$ and $B^- \to \Lambda_c^+ \bar{p} \pi^-$ BR measurements,
- Measurement of their ratio,
- BRs of B^- decays via $\Sigma_c(2455)^0$, $\Sigma_c(2800)^0$,
- $\Sigma_c(2455)^0$ spin consistent with $J^P = \frac{1}{2}^+$,
- $\Sigma_c(2455)^0$ and $\Sigma_c(2800)^0$ masses and widths measured.